Empowering extra fuel supply in *E. coli* by electron bifurcation for robust H$_2$, ATP and succinate production

Pattarawan Intasian[1], Chalermroj Sutthaphirom[1], Asweena Binlaeh[1], Jittima Phonbuppha[1], Juthamas Jaroensuk[1], Somjai Teanphonkrang[1], Thamonwan Woraruthai[1], Charndanai Tirapanampai[1], Warunya Onchan[1], Albert Schulte[1], Wolfgang Buckel[2,3], Nopphon Weeranoppanant[1,4], Thanyaporn Wongnate[1], Jeerus Sucharitakul[5] and Pimchai Chaiyen[1*]

Affiliations:

[1]School of Biomolecular Science and Engineering, Vidyasirimedhi Institute of Science and Technology (VISTEC), Wangchan Valley, Rayong, Thailand

[2]Laboratorium für Mikrobiologie, Fachbereich Biologie and Synmikro, Philipps-Universitüt, Marburg, Germany

[3]Max-Plank-Institut für terrestrische Mikrobiologie, Marburg, Germany

[4]Department of Chemical Engineering, Faculty of Engineering, Burapha University, Chonburi, 20131, Thailand

[5]Department of Biochemistry, Faculty of Dentistry, Chulalongkorn University, Patumwan, Bangkok, Thailand

*Corresponding author. Email: pimchai.chaiyen@vistec.ac.th

Abstract:

Microbial production of hydrogen (future ideal fuel and important gas for industries) under anoxic conditions has limited ATP availability and low efficiency. We engineered *E. coli* K12 to acquire a flavin-based electron bifurcation (FBEB) system, a bioenergetic route typically found in strict anaerobes, which uses NADH to generate low potential reduced ferredoxin and high potential butyryl-CoA. The oxygen-tolerant FBEB-*E. coli* showed higher H$_2$ and succinate production (2-4 folds), lower cellular reduction potentials, greater accumulation of cellular reductants and various metabolites, including ATP (up to a 7-fold increase). It could better tolerate prolonged and recycled usage of the engineered cell for H$_2$ and succinate production than the native strain. FBEB-*E. coli* could also use various substrates such as formate, D-glucose and food waste for H$_2$ and succinate production. This is a promising pathway to sustainable H$_2$ and succinate production. This work also demonstrates that *E. coli* with an extra electron bifurcation system is a robust synthetic biology host.
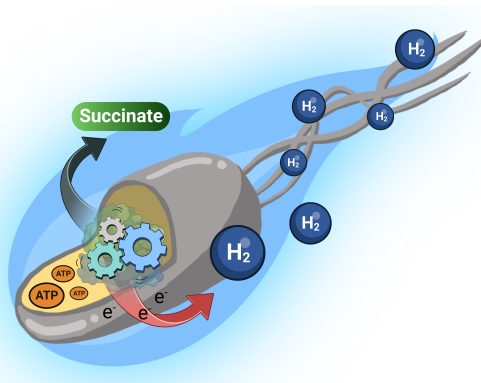
One-Sentence Summary: Rewiring FBEB-*E. coli* electron flux *via* enhancement of cellular reductants and ATP leads to significantly higher H_2 and succinate production.

5

10

15

20

25

30

35

40

45

Introduction

Hydrogen (H_2) is regarded as a promising fuel for the future because of its zero-carbon emission[1] and high energy density compared to methane, gasoline and diesel[2]. It can be used in various applications, including transportation, electricity, heat generation and chemical synthesis[3]. Global H_2 generation market is projected to grow from \$150bn in 2021 to \$220bn in 2028 (5.6% compound annual growth)[4]. However, 96% of the current global production is from fossil fuels (48% from natural gas steam reforming, 30% from crude oil partial oxidation and 18% from coal gasification)[3] *via* high temperature using metal catalysts[5]. H_2 production from these industrial processes or from recently discovered resources[6] is non-renewable and creates a large footprint of CO_2 emissions[3]. On the other hand, biological H_2 production is genuinely sustainable because the process can use renewable substrates and can be performed under mild conditions[7]. The ability of microbial cell factories to utilize low value feedstocks to produce valuable chemicals is regarded as a challenging goal for sustainable catalysis[7,8].

In biological systems, H_2 is produced by hydrogenases which can be divided into three types based on their metal content, including [Fe] (with guanylylpyridinol cofactor)-, [FeFe]- and [NiFe]-hydrogenases[9]. The two latter hydrogenases typically catalyze the reversible conversion of $2H^+$ and $2e^-$ into H_2 and require electron supply from low reduction potential reductants such as reduced flavodoxin or reduced ferredoxin (Fd^-) to fuel the H_2 production direction (**Fig. 1A**). Metabolic engineering to enhance H_2 production by hydrogenases is a highly active area of research. Recently, fusion of hydrogenases with photosynthetic system I (PSI) has resulted in 1.6-4 fold increases in hydrogen production in cyanobacteria[10,11]. Facultative anaerobes such as *Escherichia coli* are also attractive for hydrogen production because they contain O_2-tolerant hydrogenases[12]. [NiFe]-hydrogenases in *E. coli* are also involved in proton-pump and energy-coupling systems[13]. Engineering these microbes to improve H_2 production was mostly done by deleting enzymes competing for electron supplies or utilizing H_2. These, however, resulted in engineered cells weaker than the native ones in terms of growth rate and robustness, since several competitive pathways are important shunts for the cells (**Table S1**). Therefore, an alternative approach which avoids extensive gene deletion to improve H_2 production is desirable.

To sustainably boost the efficiency of compound production by *E. coli*, the level of energy currency, ATP, should be increased because it is required for maintaining various cellular activities[14]. In aerobes or facultative anaerobes, ATP is synthesized by oxidative phosphorylation (oxygen-dependent) and substrate-level phosphorylation (oxygen-independent). Although oxidative phosphorylation is more efficient than substrate-level phosphorylation, this pathway cannot operate under anoxic conditions. As a result, production of valuable compounds such as H_2 or succinates which require anaerobic conditions, often results in low productivity[15,16]. Under anaerobic conditions without nitrate, glycolysis is the main mechanism for producing ATP through substrate-level phosphorylation by phosphoglycerate kinase and pyruvate kinase; NADH produced thus needs to be reconverted into NAD^+ to continue glycolysis and ATP synthesis. Therefore, we hypothesized that increasing the rate of NADH oxidation would improve intracellular ATP production.

We hypothesized that incorporation of flavin-based electron bifurcation (FBEB), a bioenergetic system used by strict anaerobes, would be able to increase the rate of NADH oxidation and accumulation of reductant inside the cell to facilitate H_2 production. FBEB has mainly been discovered during the past decade and has emerged as a new paradigm of energy metabolism[17]. Its roles under anoxic conditions are equivalent to its well-known aerobic counterpart, quinone-based electron bifurcation (QBEB) found in cytochrome bc_1 (complex III of the oxidative phosphorylation) or cytochrome b_6f (plant photosynthesis). The FBEB system consists of a two

https://doi.org/10.26434/chemrxiv-2023-fz0lz **ORCID:** https://orcid.org/0000-0002-8533-1604 Content not peer-reviewed by ChemRxiv. **License:** CC BY-NC-ND 4.0

FAD-containing electron-transfer flavoprotein (EtfAB), butyryl-CoA dehydrogenase (Bcd), and ferredoxin (Fd)[17,18]. Its overall reaction converts NADH to generate a high reduction potential product (butyryl-CoA) through the Bcd reaction and a low reduction potential reduced ferredoxin (Fd$^-$) (**Fig. 1B**).

5   In this work, we have created for the first time, a hybrid aerobic cell with an anoxic energy system, an FBEB-*E. coli* K12, in which genes encoding for all components of FBEB from *Acidaminococcus fermentans* were incorporated into *E. coli* K12. We proposed that the hybrid FBEB-*E. coli* K12 has a dual advantage: (1) to increase H$_2$ synthesis by re-directing electron flow towards more Fd$^-$ production and (2) to boost intracellular ATP by increasing the rate of NADH oxidation *via* EtfAB (an electron transfer component of FBEB) (**Fig. 1C**). The results showed that the oxygen-tolerant hybrid FBEB-*E. coli* was indeed highly efficient and robust in H$_2$ production, generating levels of H$_2$ from formate and D-glucose ~2-4 fold higher than the native *E. coli* without affecting the growth kinetics. We analyzed the targeted metabolomics, the cellular reduction potentials and *in vitro* hydrogen-producing activities (**Fig. 1D**). Targeted metabolomics analyses showed that FBEB-*E. coli* has distinctly higher production of ATP (up to 7-fold with formate as a substrate) and dicarboxylic acids such as succinate (~2-4 fold with D-glucose as a substrate) than the native cell. We also found that FBEB-*E. coli* can produce H$_2$ and succinate from food waste with high productivity, illustrating its potential in future applications to support sustainable biotechnology (**Fig. 1E**).
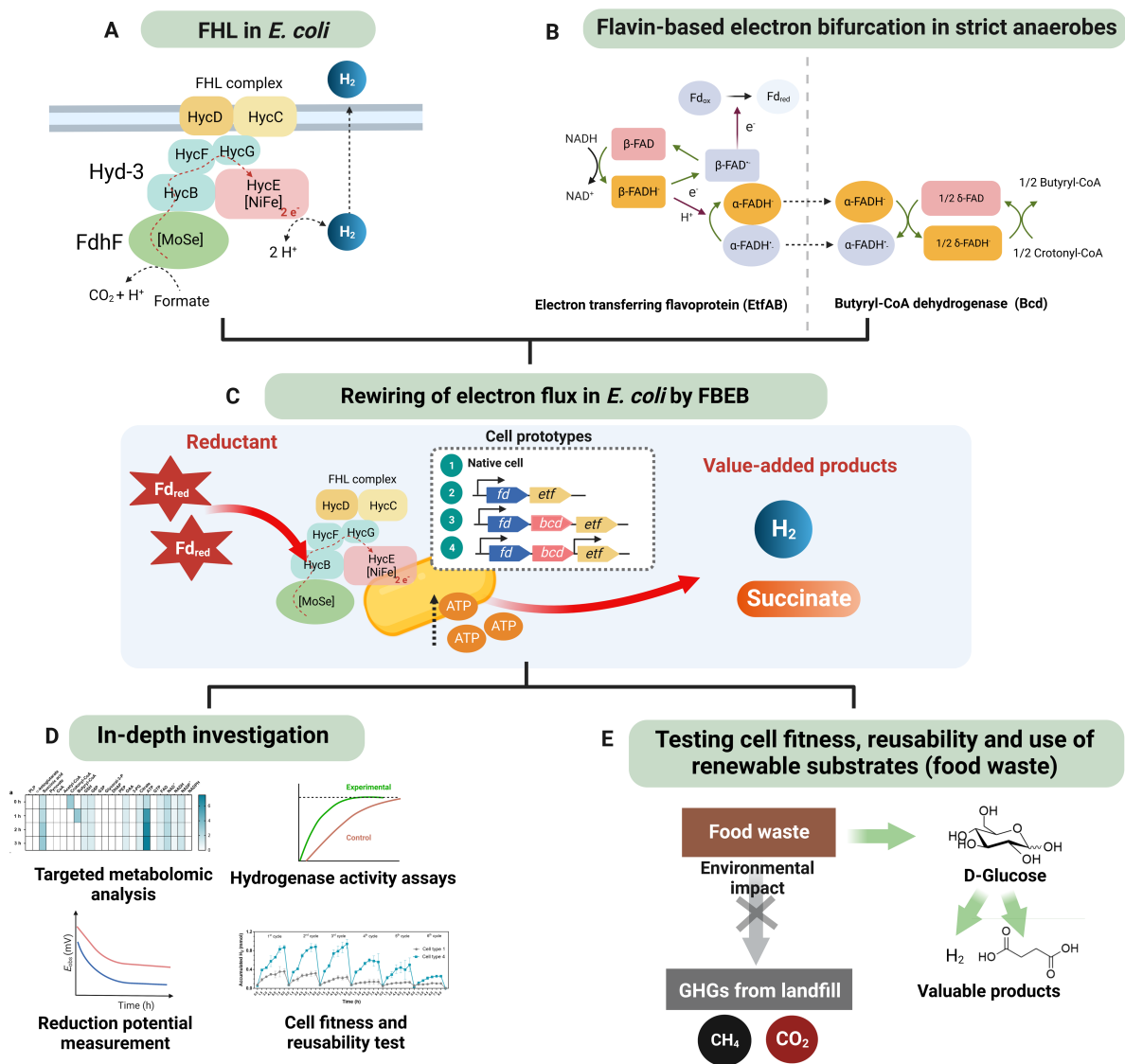
Fig. 1. Rational design of electron rewiring/boosting system in *E. coli*. (A) *E. coli* K12 contains various subunits of hydrogenase-3 (Hyd-3). Hyd-3 can receive electrons from HycF (Fd-like protein subunit) and transfer them to the H_2-generating subunit (HycE)[19]. (B) FBEB system found in strict anaerobes such as *A. fermentans* generally consists of Fd, EtfAB and Bcd. (C) The hybrid electron boosting system was created by incorporating FBEB into *E. coli* to create FBEB-*E. coli* prototypes with different promoter arrangements. (D) In-depth investigation of FBEB-*E. coli* includes targeted metabolomics, hydrogenase activity assays, reduction potential measurement and evaluation of cell fitness and reusability. (E) FBEB-*E. coli* hybrid was tested for its ability to convert food waste for H_2 production.

Results

Rational design of electron rewiring/boosting system in *E. coli*.

To generate the engineered cell with robust production of H_2 and valuable metabolites, we first incorporated the FBEB system into *E. coli K*12. FBEB components from *A. fermentans* were chosen due to their well understood mechanism[18,20] and their good expression in *E. coli* BL21-DE3[20]. In *E. coli K12*, the HycB subunit in hydrogenase-3 (Hyd-3) can receive electrons from HycF (Fd-like protein subunit) and transfer them to the H_2-generating subunit (HycE)[19]. We hypothesized that Fd^- produced from FBEB can transfer electrons to the [4Fe-4S] redox center bound in HycB which can be further used for H_2 production. We also hypothesized that adding an extra route of NADH oxidation *via* EtfAB bifurcation would promote more ATP production because keeping a low ratio of NAD^+/NADH would support continuation of glycolysis and substrate-level phosphorylation (see full explanation in **Supplementary Text**).

Three strains of FBEB-*E. coli* hybrids were constructed harboring *fd, etfAB* and *bcd* genes from *A. fermentans* into *E. coli* K12 W3110 (known H_2 producing strain) with different promoter arrangements (**Method 1**, **Fig. 1C**, **Fig. S1**, **Table S2 and Table S3)**. Expression of these proteins is shown in **Fig. S2**, and the results (using the methods in **Method 2** and **3**) showed that the FBEB-*E. coli* hybrid which overexpressed Fd, Bcd, and EtfAB under two T7 promoters (cell prototype 4, **Fig. 1C**) generates the highest H_2. For native *E. coli*, the yield of hydrogen produced is known to be ~25-50% per formate and ~25% per D-glucose used[21,22]. Our results showed that H_2 was produced with a 27.5%, 28%, 50% and 66% yield (per formate used) for the cell prototypes 1, 2, 3, and 4, respectively (**Fig. S3**). The results clearly indicate that overexpression of *fd, bcd* and *etfAB* are required for enhancing H_2 production. We thus defined the cell prototype 4 as the lead FBEB-*E. coli* hybrid and used it for further investigation in this study.

Productivity of FBEB-*E. coli* using formate as a substrate

Optimization of H_2 production from the FBEB-E. coli by adjusting pH, temperature, and CO_2 entrapment.

As pH can influence intracellular NADH/NAD^+ dynamics, reduction potentials, and physiological functions of bacteria[23], we first measured H_2 produced by FBEB- and native *E. coli* at 37 °C and various pHs (4.5 to 8) as described in **Method 4** and **Supplementary Text** . The data in **Fig. S4A** showed that pH 6.0 and 6.5 gave the best yield of hydrogen production. For temperature effects, we found that at pH 6.0, the temperature at 37 °C gave the highest yield per formate used (80%) (**Fig. S4B**).

As the removal of CO_2 would decrease the amount of product accumulated and drive the thermodynamics of the reaction towards H_2 production, we set up a CO_2-entrapping system using saturated $Ca(OH)_2$ solution to remove CO_2, a co-product from the formate hydrogenlyase (FHL) reaction (illustrated in **Fig. S4C**). We found that at 37 °C, pH 6.0 and using CO_2 entrapment, FBEB-*E. coli* gave a 100% yield of hydrogen produced from formate while the native cell only gave a 40% yield (**Fig. 2A and Fig. S5**). The amount of CO_2 produced in the air space of the cell chamber was also higher for FBEB-*E. coli*, showing a similar trend as H_2 production (**Fig. 2B**), confirming that the increased amount of H_2 in the engineered cell was produced through FHL activities, which generate H_2 and CO_2 from formate equivalently.

https://doi.org/10.26434/chemrxiv-2023-fz0lz **ORCID:** https://orcid.org/0000-0002-8533-1604 Content not peer-reviewed by ChemRxiv. **License:** CC BY-NC-ND 4.0

An advantage of using *E. coli* for producing H_2 is that cells can be grown under aerobic conditions, allowing fast biomass production and convenient culture. To initiate H_2 production, the culture is normally switched to anaerobiosis conditions to maximize activities of hydrogenases after adding lactose to induce expression of FBEB. We tested the ability of FBEB-*E. coli* to tolerate oxygen by re-exposing FBEB-*E. coli* to air for 0.5, 1, 2 and 4 hours (as described in **Method 4**). The systems were then purged with N_2 for 30 minutes to reactivate hydrogenase activities and H_2 production was measured in comparison to the condition under strict anaerobiosis. The results clearly showed that the oxygen exposure did not affect H_2 production by FBEB-*E. coli* (**Fig. S6**). All systems showed similar levels of H_2 production, indicating that FBEB-*E. coli* can tolerate oxygen well and should allow feasible design for H_2 production in the future.

Mechanisms underlying the superior H_2 production.

Identification of changes in metabolites of FBEB-E. coli using targeted metabolomics

To investigate further into the mechanisms underlying the improvement of H_2 production in FBEB-*E. coli*, 30 metabolites related to targeted pathways when using formate as a substrate were analyzed (**Supplementary Data S1**). **Fig. 2C** shows metabolomics data analyzed by two-way ANOVA. The heatmaps display levels of 24 compounds (excluding fatty acids) found in FBEB-*E. coli* compared to the native *E. coli* at 0-3 hours. Absolute concentrations of compounds displaying high ratio differences are shown in **Fig. 2D**. We also measured concentrations of selected fatty acids (propionate, tetradecanoate and octadecanoate) (**Fig. 2E**).

The results indicate that the incorporated FBEB functions in *E. coli* K12 as expected. Metabolites in the glycolysis and the tricarboxylic acid (TCA) cycle such as citrate and glucose-6-phosphate are similar between the two cell types, implying that FBEB does not interfere with these two pathways when formate was used as a substrate. However, FBEB-*E. coli* displayed much higher levels of ATP, NAD^+ and succinate than the native *E. coli,* while NADH and NADPH were lower in the FBEB-*E. coli* than in the native *E. coli*.

We noted the distinctively high level of ATP (see chromatogram in **Fig. S7**) in FBEB-*E. coli,* which was ~2-times higher at 0 hour, 3-times higher at 1 hour, and 7-times higher at 2 hours. This ATP enhancement might be explained by two plausible mechanisms. The first mechanism is possibly from the presence of a low ratio of $NADH/NAD^+$ (0.1 at 1 hour and 0.22 at 3 hours) in FBEB-*E. coli*. Under anaerobic conditions, the $NADH/NAD^+$ ratio is typically ~0.7 due to low NAD^+ regeneration which is different from the $NADH/NAD^+$ ratio of <0.1 found under regular aerobic conditions where ATP production is active[24]. We propose that in FBEB-*E. coli*, which contains the extra NADH oxidation pathway provided by EtfAB to keep the level of $NADH/NAD^+$ at ~0.1-0.22, ATP production is promoted by substrate-level phosphorylation in glycolysis. The second mechanism possibly can be attributed to the high level of H_2 in FBEB-*E. coli* which can be oxidized by hydrogenases (possibly types 1 and 2 in *E. coli*) to create an electrochemical gradient of H^+, leading to ATP synthesis by the H^+/K^+ pump and ATPase (involving ATP hydrolysis/synthesis and transportation of ions across the membrane of cells)[25].

Interestingly, FBEB-*E. coli* produced a significantly higher level of succinate (a valuable compound for industry) than the native *E. coli*. Normally, succinate is produced through the reductive branch of the TCA cycle, the glyoxylate pathway and the oxidative TCA cycle. The reductive branch produces succinate by coupling phosphoenolpyruvate (PEP) and CO_2 to produce oxaloacetate (OAA) as a starting compound. As our analysis (**Fig. 2C**) did not detect significant differences in OAA between the two cell types, the high amount of succinate produced by FBEB-

E. coli may also come from other metabolic shunts. H_2 produced from formate was previously reported to enhance succinate production[26]. We propose that H_2 can be oxidized by Hyd-2 to generate a proton gradient. HybB which is the integral membrane subunit of Hyd-2 can then convert oxidized menaquinol (MK) to MKH_2 (reduced form). The resulting MKH_2 is then re-oxidized by fumarate reductase to convert fumarate into succinate[26], increasing the level of succinate production in FBEB-*E. coli*.

FBEB-*E. coli* showed higher levels of crotonyl-CoA at 0 hour and butyryl-CoA at 1 hour than the native *E. coli*; these data may be linked to the higher amounts of long chain fatty acids produced by FBEB-*E. coli*. The native *E. coli* contains thiolases[27] and a bifunctional *fadB* gene encoding for 3-hydroxyacyl-CoA dehydrogenase/enoyl-CoA hydratase[28] that catalyze production of crotonyl-CoA from acetyl-CoA[28]. The system provides a high potential electron acceptor crotonyl-CoA for FBEB to function inside *E. coli*. The data in **Fig. 2D** indicate that at the beginning of H_2 production in FBEB-*E. coli*, crotonyl-CoA was converted into butyryl-CoA which decreased later. The decreased level of butyryl-CoA at the later time points implies that the compound is used for downstream synthesis of other metabolites. The data (**Fig. 2E** and **Fig. S8**) showed that FBEB-*E. coli* produced higher amounts of long chain fatty acids such as tetradecanoate, hexadecanoate and octodecanoate while the native *E. coli* produced higher amounts of proprionate. Butyrate could not be detected in either strain, consistent with the previous work which found that butyrate could not be detected in the native *E. coli*[29]. We propose that the extra synthesis of butyryl-CoA *via* the FBEB system supports fatty acid synthesis. For the native *E. coli* with no extra synthesis of butyryl CoA, the pathway towards biosynthesis of propionate is more active. This is possibly linked to production of succinate and succinyl-CoA intermediates *via* the TCA cycle (in order to synthesize GTP) as previously reported[30]. Full analysis of the targeted metabolomics of the two cell systems are described in the **Supplementary Method 1**.

Measurement of cellular reduction potentials

We next measured the cellular reduction potentials (E_h) of FBEB-*E. coli* compared to the native *E. coli*. We expect that E_h in FBEB-*E. coli* would be lower than the native one because of the increase of Fd^- reductant and the low ratio of $NADH/NAD^+$ in the system. It was previously reported that alteration of levels of reductants and oxidants such as $NADH/NAD^+$, $NADPH/NADP^+$, 2GSH/GSSG and ubiquinone$_{red}$/ ubiquinone$_{ox}$ ratios can influence cellular E_h[31]. We also propose that lowering of E_h would facilitate formation of H_2 by hydrogenases.

We determined E_h using a redox probe and addition of redox mediators (**Supplementary Method 2**). System reduction potentials (E_{sys}) of the native *E. coli* and FBEB-*E. coli* after protein overexpression were −48.9 mV and −108.3 mV, respectively. During bioconversion, the E_{sys} of the FBEB-*E. coli* remained ~ 50-60 mV more negative than the native *E. coli* throughout 3-hours (**Fig. 2F**). These results are explained more in detail in the **Supplementary Text**. These observations clearly confirm the ability of FBEB to decrease the overall reduction potential of *E. coli*, possibly due to the high accumulation of reductants. This type of cellular physiology would facilitate H_2 production. It should be noted that the lower reduction potential may also indirectly support ATP formation due to the change of proton motive force. It was previously reported that ATPase activity and membrane proton conductance increase when E_h decreases[32].

Altogether, the results from targeted metabolomics and redox potential measurement have clearly elucidated that the increase of H_2, ATP and succinate inside FBEB-*E. coli* was indeed due to the activities of FBEB which enables the cell to possess an extra energetic path to operate under anaerobic conditions and in turn enhance production of H_2, ATP and succinate in *E. coli* (illustrated in **Fig. 2G**).
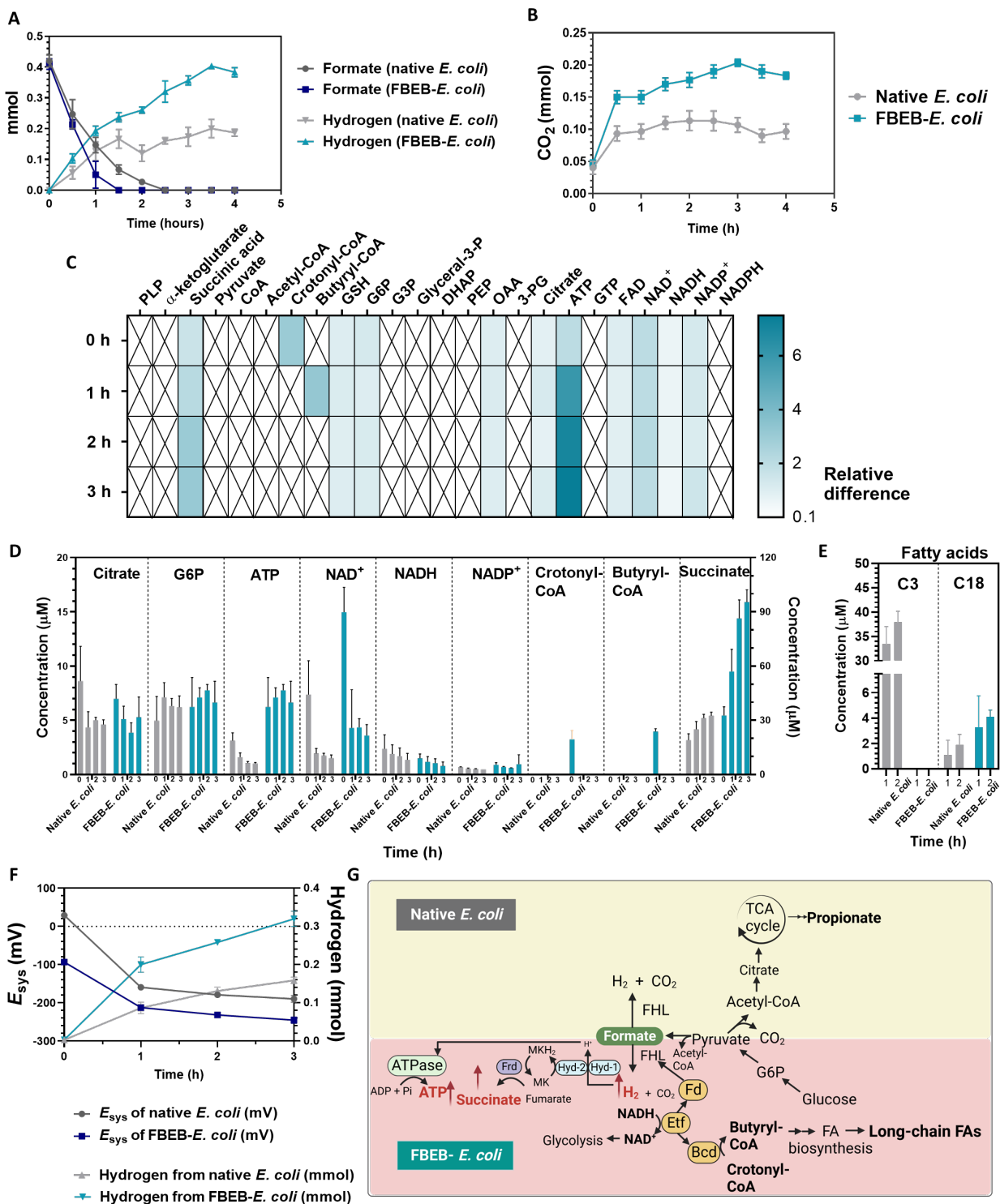
Fig. 2. Mechanisms underlying the superior H_2 production. (A) and (B) H_2 and CO_2 produced under the optimum conditions. (C) Comparison of intracellular metabolites from FBEB- and native *E. coli* at 0- and 3-hours during the bioconversion process. All metabolite standards were selected from the pathways involved. The first group is related to glycolysis (G6P, G3P, DHAP, PEP, 3-phosphoglycerate and pyruvate), and the second group consists of compounds involved in the TCA cycle (OAA, citrate, acetyl-CoA, α-ketoglutarate and succinate). The third group are compounds

involved in FBEB reactions, including NADH, crotonyl-CoA and butyryl-CoA. The fourth group includes ATP and GTP, while the fifth group are common cofactors including FAD, NAD^+, NADH, $NADP^+$, NADPH, GSH, PLP and CoA. The last group consists of compounds related to fatty acid synthesis pathways (glycerol-3-phosphate, propionate, butyrate, decanoate, tetradecanoate, hexadecanoate and octadecenoate). Among the 24 compounds, only 12 compounds were detected in the intracellular extract. The undetectable compounds (displayed by cross signs) possibly existed at very low levels under anaerobic bioconversion process (below the limit of detection). The magnitude of the difference ratio between the two cell types is represented by the intensity of the blue color on the heat map. (D) Concentrations of detected metabolites are shown on the left axis except for succinate which are shown on the right axis. (E) Short-chain (propionate) and long-chain (tetradecanoate and octadecenoate) fatty acids concentrations detected at 1 and 2 hours are shown in the right panel. (F) E_{sys} of native *E. coli* and FBEB-*E. coli* during H_2 production. (G) Proposed mechanisms underlying the boosting of electron flows in FBEB-*E. coli*.

Investigation of hydrogenase activities and reductants accumulated inside FBEB-E. coli and native E. coli

To validate that incorporated FBEB did not interfere with endogenous expression of hydrogenases, we measured *in vitro* hydrogenase activities in the supernatants of native- and FBEB-*E. coli* lysates (as described in **Supplementary Method 3**, **Fig. 3A** and **Supplementary Text**). Using sodium dithionite as a reducing agent and methyl viologen (MV) as an electron mediator, the same H_2 levels were observed in both cell lysates (**Fig. 3B**). The data indicate that both cell types expressed the same level of hydrogenases, and FBEB did not interfere with the hydrogenase expression.

We then measured the reductants accumulated inside the cell which can facilitate the formation of H_2. Formate was added into both cell lysates, and H_2 was measured. FBEB-*E. coli* lysate produced twice the levels of H_2 of the native *E. coli*, similar to the ratio of H_2 production *in vivo* (**Fig. 2A**). This indicates that the lysate of FBEB-*E. coli* contains more reducing equivalents to produce H_2, possibly in the form of Fd^-. We further added NADH and crotonyl-CoA and compared it to the reaction with only formate added (**Fig. 3C**). The results did not show an increase in H_2 compared to the system with only formate added, implying that after cell lysis, FBEB cannot catalyze the electron transfer reaction to accumulate more of the reductant (Fd^-) for H_2 enhancement as it could *in vivo* (**Fig 3D**). Therefore, the advantage of FBEB anoxic energy metabolisms to enhance H_2 production is best done *in vivo*. This possibly is attributable to the enhancement of FBEB through lowering of cellular reduction potentials and oxidation of H_2 in association with ATPase activity and modified H^+ gradient as explained in the previous section.
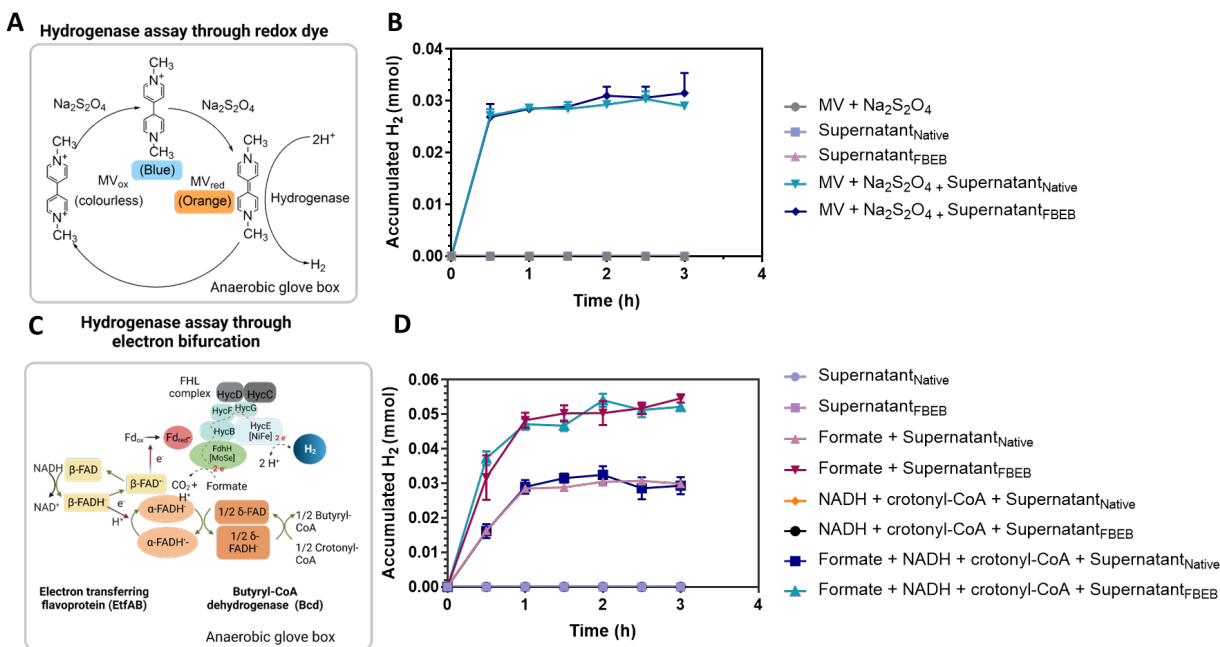
Fig. 3. *In vitro* assays of hydrogen production by supernatant from FBEB-*E. coli* and native *E. coli* lysates. (A) Hydrogenase assay through redox dye (B) *In vitro* H_2 production using MV reduced by sodium dithionite. (C) The hydrogenase assay through electron bifurcation (D) *In vitro* hydrogen production activity using electrons from various types of cell lysates. The negative controls were supernatant from lysates of native *E. coli* and FBEB-*E. coli* without formate addition. Formate was added into the system to observe H_2 produced by both cell lysates. NADH, crotonyl-CoA and formate were added into the reactions of lysates of FBEB-*E. coli* and native *E. coli* to compare with the system with only formate added.

FBEB-*E. coli* has superior cell fitness than native *E. coli.*

We next compared the recyclability and growth kinetics of FBEB-*E. coli* and native *E. coli.* In the past, most of the H_2 enhancement in bacteria were accomplished by deleting multiple genes, generally resulting in negative effects on cell fitness[16]. These engineered cells thus have not been able to demonstrate their real production capability including such things as a prolonged bioconversion process or cell recyclability[15,33]. Herein, we tested cell recyclability by growing both cells in comparison and monitoring H_2 production under anaerobic conditions for 9 hours per cycle (adding formate every 3 hours) (**Supplementary Method 4**).

The cell suspension was prepared as shown in **Fig. 4A**. The results indicate that FBEB-*E. coli* could maintain 100% H_2 productivity without adding any carbon source (except formate substrate) for up to 3 cycles, while the productivity of native *E. coli* was affected significantly since the second cycle (**Fig. 4A**). Hydrogen was produced at an 83% yield by FBEB-*E. coli* which was 4-times higher than the native cell (19% yield) at the third cycle. After five recycling cycles, the H_2 production and productivity of FBEB-*E. coli* was around 60% compared to the first cycle and its activity was 5-times better than the native *E. coli* which was severely affected after three cycles (**Fig. 4B**). These results clearly showed that FBEB helped improve hydrogen production and promoted cell endurance. When comparing growth kinetics of both cell types by measuring cell viability using colony forming units (CFU) assays, the results showed that the growth kinetics of FBEB-*E. coli* and native *E. coli* were similar (**Fig. 4C**). Altogether, these results clearly

11

demonstrate that the addition of the FBEB system into *E. coli* does not affect its growth kinetics but rather creates the engineered cell with superior H_2 production and cell fitness which is more suitable for future industrial applications.
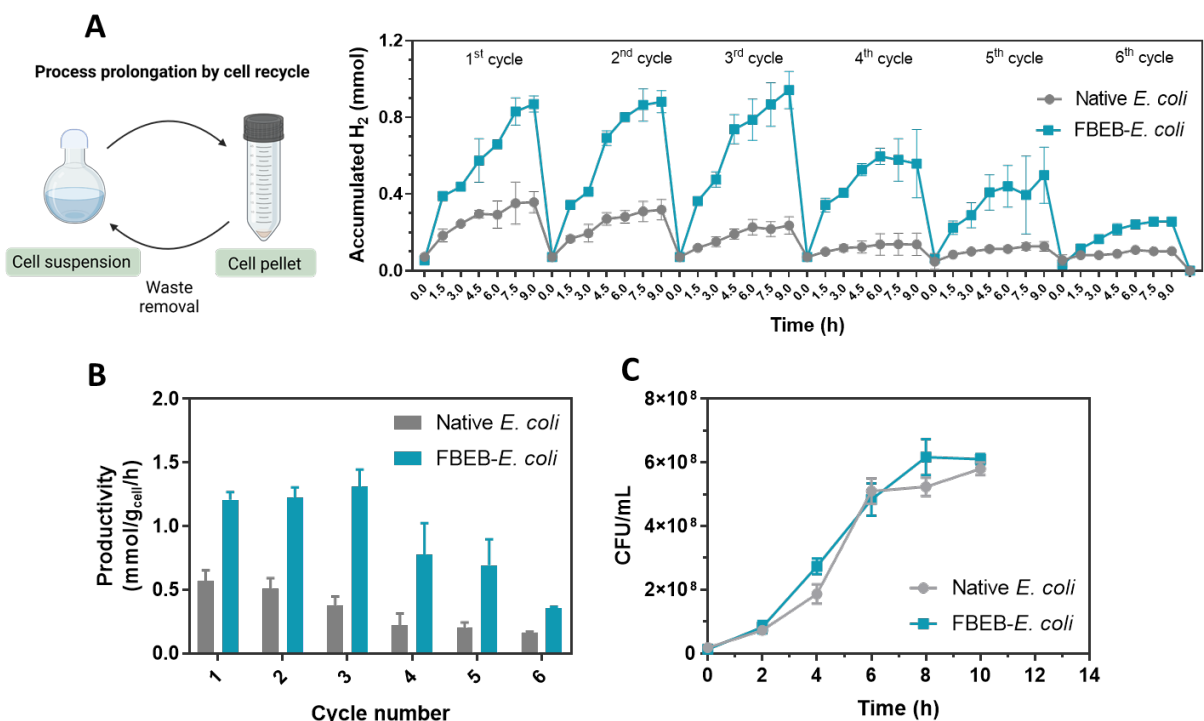

Fig. 4. Comparison of cell fitness between FBEB-*E. coli* and native *E. coli*. Hydrogen productivity at various cell recycling stages is shown in (A) and (B), respectively. Cell growth kinetics measured by colony forming unit (CFU) is shown in (C).

Analysis of targeted metabolomics of FBEB-*E. coli* using D-glucose as a substrate for H_2 and succinate production

As D-glucose is an abundant, low-cost carbon source, we investigated H_2 production and targeted metabolomics from D-glucose as described in **Supplementary Method 1**. From 4 mM D-glucose (0.24 mmol), FBEB-*E. coli* produces 0.22 mmol H_2 (45.8% yield), which was 1.83-times higher than the native *E. coli* (0.12 mmol or 25% yield) (**Fig. 5**). To investigate the effects of the FBFB system in *E. coli*, 38 metabolites (**Supplementary Data S1**) were used for targeted metabolomics analysis. Full explanation of the analysis is described in **Supplementary Text**.

Almost all metabolites in the glycolysis were up-regulated in FBEB-*E. coli* compared to native *E. coli*. FBEB-*E. coli* utilized D-glucose faster and produced higher amounts of G6P, 3-phosphoglycerate, PEP and pyruvate than the native *E. coli*. These data were consistent with a lower ratio of $NADH/NAD^+$ in FBEB-*E. coli* than in native *E. coli* at 0-1 hours, promoting the continuation of glycolysis enzymes activities. However, after 3 h, the $NADH/NAD^+$ ratio of FBEB-*E. coli* rose to be higher than native *E. coli*, possibly because reducing equivalents in the FBEB-*E. coli* system reached a sufficient level for H_2 production.

For metabolites in mixed-acid fermentation, FBEB-*E. coli* utilized formate faster than the native cell. The amount of succinate produced in FBEB-*E. coli* is very high (3.53 mM) (see chromatogram in **Fig. S9**) and much higher than the results when using formate as substrate at 2

hours (5.2-fold). This is probably because D-glucose can be metabolized to form pyruvate, a carbon precursor for succinate production.

Levels of all amino acids analyzed except valine and leucine were similar between FBEB-*E. coli* and native *E. coli*. The levels of valine and leucine in FBEB-*E. coli* were found to be higher than the native cell, possibly due to the increase of their precursors i.e. pyruvate. These data indicate that cell fitness in FBEB-*E. coli* is not affected but rather better than that of *E. coli*.

Interestingly, the acetate level in FBEB-*E. coli* is much lower than in native *E. coli*. It implies that acetate shunt was not activated in FBEB-*E. coli*, possibly due to enough ATP being produced. This effect is advantageous because the high acetate concentration can inhibit cell growth[34]. Using D-glucose as a substrate, ATP was undetectable in both cell types, in agreement with previous literature noting that the ATP level in fermentative cells is generally very low[35]. Nevertheless, the low level of acetate and the active production of H_2 and succinate in FBEB-*E. coli* indicates that its ATP level is sufficient.

The lactate level in FBEB-*E. coli* was also lower than in native *E. coli*, indicating that the lactate shunt to regenerate NAD^+ was not very active. Generally, lactate is produced by LDH to regenerate NAD^+ to continuously drive synthesis of ATP from glycolysis[36]. The low amount of lactate in FBEB-*E. coli* strongly suggests that the rate of NADH oxidation is enough.

Altogether, the FBEB system from strict anaerobes can function well inside *E. coli* as an extra energy supply system to generate sufficient ATP, maintain high levels of metabolites necessary for cell growth and fitness and result in high production of succinate. Therefore, FBEB-*E. coli* demonstrates a proof-of-concept of incorporating an extra energy system in metabolic engineering for boosting efficiency and robustness of a whole cell biocatalyst.
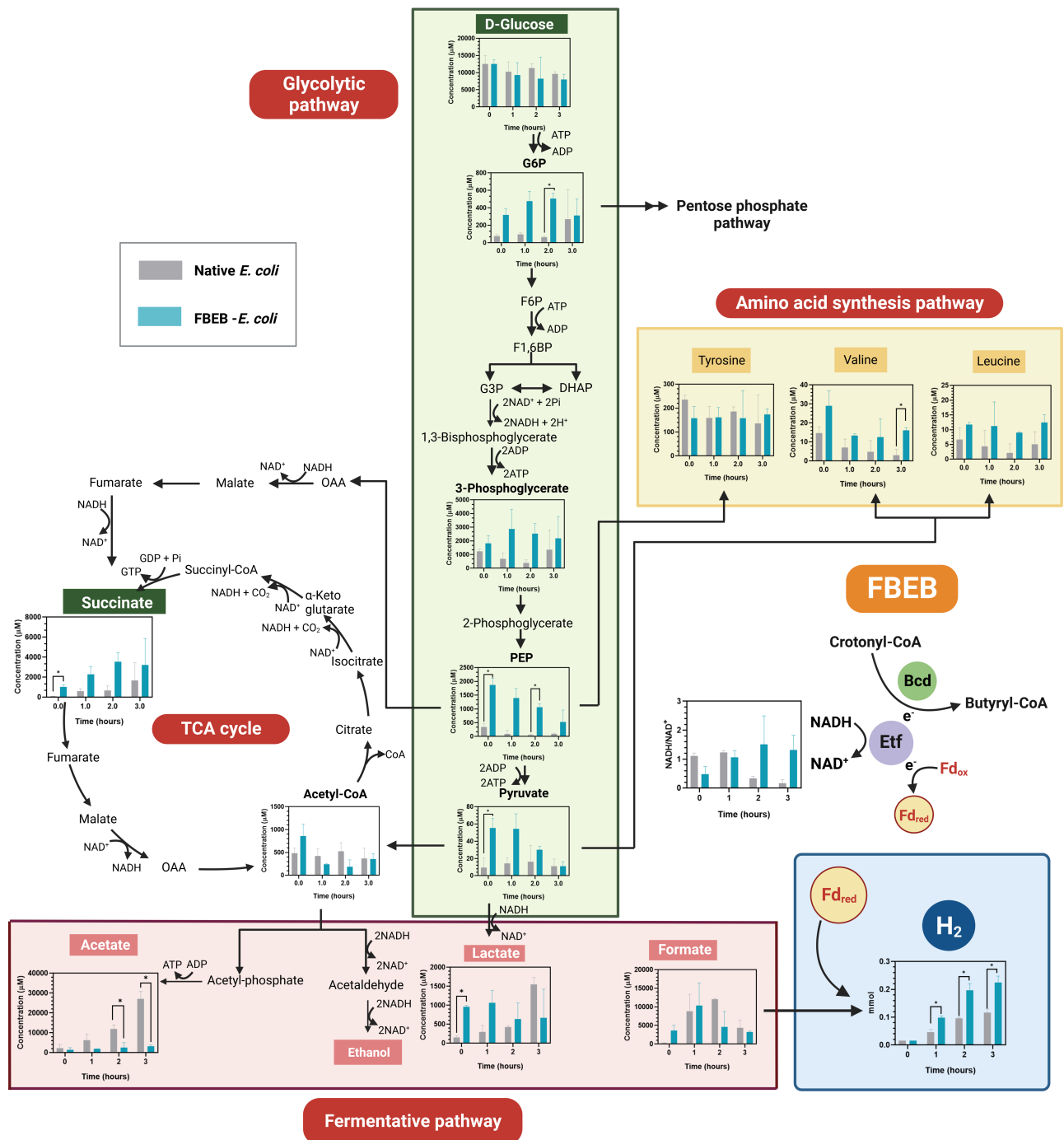
Fig. 5. Changes of intracellular metabolites analyzed by targeted metabolomics using D-glucose as a substrate. Intracellular metabolites of native *E. coli* and FBEB-*E. coli* were analyzed between 0 and 3 hours.

5

Ability of FBEB-*E. coli* to produce hydrogen from heterogenous and ubiquitous substrates (food waste)

Food waste management is a key environmental issue globally because it is generated at a rate of around 1.03 billion tons per year[37]. Its disposal in landfills contributes to air and water pollution and 14.5% of overall methane emission[38] (**Fig. 6A**). As food waste contains a high content of D-glucose as well as other compounds, we therefore explored the ability of the FBEB-*E. coli* cell to produce H_2 and succinate from food waste.

Food waste was first hydrolyzed into D-glucose by 2.5% phosphoric acid, and the resulting mixture was sterilized to inhibit the growth of natural microbes (**Supplementary Method 5**) and the substrate concentrations were optimized (**Fig. S10**). The bioconversion using FBEB-*E. coli* and native *E. coli* were carried out with the same amount of pretreated food waste (equivalent to 0.1 mmol D-glucose) added into the system every 3 hours. The results (**Fig. 6B**) showed that FBEB-*E. coli* could produce 0.43 mmol H_2 from 0.6 mmol D-glucose in food waste with the high productivity (0.375 mmol H_2/g dry cell weight/hour during 6-9 hours) compared to the native *E. coli* which could only produce H_2 of 0.2 mmol from 0.6 mmol D-glucose in food waste with H_2 productivity of 0.12 mmol H_2/g dry cell weight/h during 6-9 hours (**Fig. 6C**). FBEB-*E. coli* also produced 2.5 times higher succinate than of the native-*E. coli* (**Fig. 6D**). Altogether, these results clearly demonstrate the robustness and efficiency of FBEB-*E. coli* for using food waste as feedstock to generate high value products such as H_2 and succinate. Our work herein also presents a promising and sustainable technology to convert problematic organic waste into valuable products, fully aligned with a circular and green economic model.
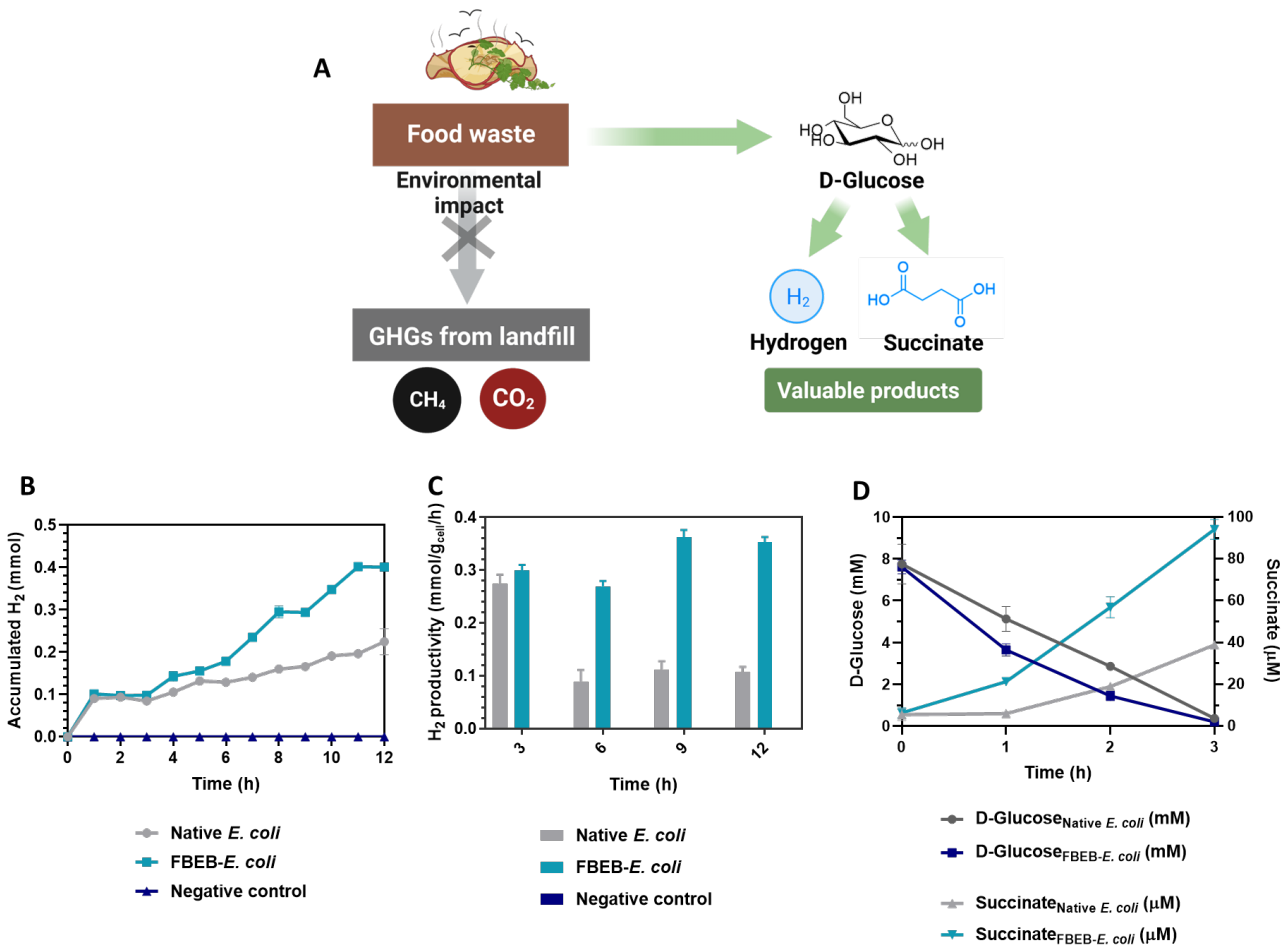
Fig. 6. Exploring the ability of FBEB-*E. coli* to produce H_2 and succinate from food waste. Hydrogen production using food waste as a substrate (A). Accumulated hydrogen (B) and productivity (C) were measured during 12-h bioconversion. D-Glucose consumption and succinate production from food waste is shown in (D).

Discussions and conclusion

Our work demonstrates for the first time that by incorporating the FBEB energy system commonly found in strict anaerobes into oxygen-tolerant *E. coli*, a hybrid FBEB-*E. coli* with high productivity of H_2 and succinate production and optimal cell robustness could be obtained. Because the midpoint potential (E_m) of FBEB is about 400 mV more negative than that of QBEB[17], the addition of FBEB would also lower the cellular reduction potential and increase the pool of Fd^- which can serve as reductant for the FHL complex of *E. coli* to produce H_2. Analyses using reduction potential measurement, hydrogenase activity assays and targeted metabolomics have shown that these metabolic enhancements are achieved through extra accumulation of cellular reductant, enhanced NADH oxidation by EtfAB and increased levels of cellular ATP. FBEB-*E. coli* can use various compounds such as formate, D-glucose and food waste as substrates.

The FBEB-*E. coli* system is among the best metabolically engineered oxygen-tolerant facultative anaerobes for H_2 production in terms of yield, cell growth and robustness (**Table S1**), possibly due to the extra fueling effects by the incorporated FBEB (**Fig. 2**). Although the system still cannot produce H_2 as high as *Clostridia*[39], its ability to grow under aerobic conditions offers an advantage for scaling up in the future. The tolerance of the *E. coli* system towards oxygen

16

exposure without the requirement of light input also offers an advantage over H_2 production by cyanobacteria which is sensitive to oxygen inactivation and requires light for growth[40].

The increased cellular reductant (Fd_{red}) and the lowering of E_h in FBEB-*E. coli* is possibly linked to the FHL complex or Hyd-3 to synthesize H_2. FHL shares a sequence similarity with the membrane-bound hydrogenases *Pyrococcus furiosus*, which is known to accept electrons from reduced Fd[41]. It was previously shown that the fusion of *E. coli* Hyd-3 with *Thermotoga maritima* Fd could lead to more H_2 production when co-expressed with *T. maritima* pyruvate-ferredoxin oxidoreductase (PFOR)[42].

The ability of FBEB to boost up cellular levels of ATP highlights its potential to be used as a generic tool for other synthetic biology systems in the future. We proposed that the ATP boosting by FBEB is linked to activities of H_2 oxidizing hydrogenases and H^+/K^+ ATPase. It was previously reported that the increased H_2 can cause a higher ratio of $2H^+/K^+$[43]. When *hypF* (the maturation factors for Hyd-1, 2 and 3) was mutated to disrupt production of hydrogenases, total ATPase activity was decreased ~27% at pH 7.5 and ~45% pH 5.5[44]. Production of cellular or *in vitro* ATP is desirable for biocatalysis and synthetic biology. Although *in vitro* ATP regeneration can be simply done using reactions of kinases and phosphate donors such as PEP, acetyl phosphate or polyphosphate[45], enhancing *in vivo* ATP is more complicated because it involves various reaction components, pH control (ATP/ADP ratio can be enhanced under acidic conditions), and requires controlling of the respiratory chain reactions[46]. Therefore, the ability of the FBEB system to increase cellular ATP makes it attractive as a generic synthetic biology tool to boost up cellular ATP in other metabolically engineered cells which is required to be operated other anaerobic fermentation processes in the future.

Our results presented herein also demonstrate the ability of FBEB-*E. coli* to produce succinate, one of the top 10 biochemicals for the future[47]. In the past, several natural facultative anaerobes or aerobes such as *Actinobacillus succinogenes*, *Basfia succiniciproducens* and *Aspergillus niger* could be used to produce high titers of succinate[48]. *A. succinogenes* 130Z produces succinate from xylose up to 0.78 g/g D-xylose or 39.6 g/L within 1550 hours[49] while *B. succiniciproducens* produces succinate up to 1.02 g/g glycerol or 5.21 g/L titer within 80 hours under anaerobic conditions[50]. Our system here could produce 3.5 mM succinate from 5 mM D-glucose (equivalent to 0.65 g/g D-glucose or 4.13 g/L titer) within only 3 hours. Although the yield and titer of FBEB-*E. coli* are less than the industrial strains, the production rate of FBEB-*E. coli* is much faster. It should be noted that the current FBEB-*E. coli* has not been engineered to produce succinate as the main product. With proper metabolic engineering for succinate production, FBEB-*E. coli* should hold its promise for robust production of succinate in the future.

Altogether, we have shown that FBEB-*E. coli* is among the best metabolically engineered oxygen-tolerant bacterial H_2 production system reported to date. The system also provides the dual advantages of hydrogen and succinate production from renewable sources such as D-glucose and food waste. The system's ability to increase cellular ATP levels also paves the way for the future to explore more applications of FBEB, a conserved energetic system from anaerobes, with oxygen-tolerant cells. We envision that empowering oxygen-tolerant cells with FBEB is equivalent to providing cells with an extra fuel engine to cope with cellular energy manipulations under anoxic conditions.

Materials and Methods
Materials

All laboratory chemicals were purchased from Tokyo Chemical Industry (TCI), Sigma-Aldrich, Merck or HiMedia. For molecular biology work, *E. coli* XL1-Blue was used as a host for plasmid preparation. Restriction enzymes, T4 DNA ligase, PCR kits, plasmid extraction kits, Gibson Cloning kits, and other molecular biology reagents were purchased from FAVORGEN or New England Biolabs (NEB). DNA sequencing was performed by 1st BASE DNA Sequencing Service (Malaysia). *E. coli* K12 W3110 (ATCC® 27325TM) purchased from American Type Culture Collection (ATCC) was used for whole-cell production of H_2 and for analysis of intracellular metabolites. pET11a and pUC18T-mini-Tn7T-Gm were used for plasmid construction. The construction of plasmids used in this study is described in Methods.

Methods

1. Construction of pUC18T-*fd-etfAB-rnap*, pUC18T-*fd-bcd-etfAB-T7-rnap* and pUC18T-*fd-bcd-T7-etfAB-rnap* plasmids

The overall constructs of expressions systems are illustrated in Fig. S1. *E. coli* K12 W3110 was used as the cell prototype 1. *fd*, *etfA, etfB* and *bcd* genes from *A. fermentans* (NCBI Reference Sequences WP_012938723.1, UEA72443.1, UEA72444.1 and UEA71549.1) were used for expression of ferredoxin, electron transfer flavoprotein (subunit alpha and beta) and butyryl-CoA dehydrogenase, respectively in *E. coli* K12 W3110. For plasmid construction, the pET11a-*etfAB* plasmid was digested by XbaI, and the *fd* gene was amplified using *fd1*_F and *fd1*_R as primers for PCR (Table S2). Next, *fd* was assembled with pET11a-*etfAB* using a Gibson assembly kit to yield the pET11a-*fd-etfAB* plasmid. Then, the pET11a-*fd-etfAB* plasmid was amplified spanning from the position of T7 promoter (in front of *fd*) to T7 terminator to obtain a DNA piece spanning the T7 promoter through *fd-etfAB* gene and the T7 terminator using *T7-fd-etfAB-T7ter*_F and *T7-fd-etfBA-T7ter*_R primers. The resulting DNA product was assembled into pUC18T-mini-Tn7T-Gm containing a T7 RNA polymerase which was pre-digested by PstI to yield the pUC18T-*fd-etfAB-T7-rnap* plasmid (the plasmid for the cell prototype 2).

For constructing the plasmid of the cell prototype 3 (pUC18T-*fd-bcd-etfAB-T7rnap*), the pET11a-*etfAB* plasmid was digested by XbaI. Then, *fd* was amplified using *fd2*_F and *fd2*_R primers, and *bcd* was amplified using *bcd*_F and *bcd*_R as primers in PCR (Table S2). These two pieces of genes were assembled with pET11a-*etfAB* using a Gibson assembly kit to yield the pET11a-*fd-bcd-etfAB* plasmid. The pUC18T-mini-Tn7T-Gm containing T7 RNA polymerase was then digested by PstI, and the *fd-bcd-etfAB* gene piece was amplified from the pET11a-*fd-bcd-etfAB* using *T7-fd-bcd-etfAB-T7ter*_F and *T7-fd-bcd-etfAB-T7ter*_R as primers. Lastly, the DNA product was assembled into pUC18T-mini-Tn7T-Gm-*T7RNAP* using a Gibson assembly kit.

For constructing the plasmid of cell prototype 4 (pUC18T-*fd-bcd-T7-etfAB-T7rnap*), pUC18T-mini-Tn7T-Gm containing T7 RNA polymerase was cut by PstI. A DNA product of the *T7 promoter-fd-bcd* was then amplified from the pUC18T-*fd-bcd-etfAB-T7rnap* plasmid using *T7 promoter-fd-bcd*_F and *T7 promoter-fd-bcd*_R as primers for PCR (Table S2). Another *T7 promoter* gene was then amplified using *T7 promoter*_F and *T7 promoter*_R primers. The gene encoding for *EtfAB* was amplified using *etfAB*_F and *etfAB*_R primers. After that, these three pieces of DNA products were assembled with pUC18T-mini-Tn7T-Gm-*T7RNAP* using a Gibson

18

assembly kit to yield the pUC18T-*fd-bcd-T7-etfAB-T7rnap plasmids*. All steps for constructing the overexpression systems are illustrated in Fig. S1.

2. Preparation of *E. coli* whole-cell biocatalyst and bioconversion process

The recombinant plasmids (15 ng) were transformed into *E. coli* K12 W3110 and the cells were grown on an LB agar plate at 37 °C for 16-18 hours using 100 μg/mL ampicillin selection. Then, a single colony was inoculated into LB broth supplemented with carbon source and other necessary elements (30 mM D-glucose, 2 μM sodium selenite, 2 μM ammonium molybdate and 500 μM nickel (II) chloride). The culture was shaken at 37 °C for 16-18 hours under aerobic conditions. Then, 1% starter was inoculated into 80 mL of LB broth supplemented with metal elements at the same concentrations as the starter (except D-glucose). This culture was then removed oxygen by equilibrating a solution in an anaerobic glove box. The container was capped and shaken at 37 °C until the OD_{600} reached 0.6-0.8. Then, 1 mM lactose was added to induce protein expression and the cells were further grown under anaerobic conditions for 8 h. After that, the culture was centrifuged at 4 °C, 3900 × g for 20 min and used for a bioconversion process. The resulting pellet was resuspended in 100 mM potassium phosphate buffer pH 6 and adjusted OD_{600} of the suspension to 2. Next, either formate or D-glucose was added into the cell suspension as a substrate in a 60 mL capped vial. The reaction was shaken at 37 °C at 220 rpm. Then, hydrogen gas was analyzed using GC-TCD, formate was analyzed using HPLC-DAD, and D-glucose was analyzed using HPLC-RID.

3. Product and substrate analysis

Hydrogen gas in the head space of the reaction was taken at various time points to analyze levels of H_2 and CO_2 using GC-TCD. Gas volume was measured using 50 mL syringes. Hydrogen gas was analyzed using GC-TCD with a CP-Mol Sieve 5A column from Agilent. Nitrogen gas was used as a carrier gas with a flow rate of 4 mL/min. An injection temperature of 120 °C and detector temperature of 250 °C were used. The oven temperature was set at 40 °C with holding for 3 min. For formate and D-glucose detection, 1 mL cell suspension was centrifuged at 4 °C, 3900 × g for 20 min. The supernatant was filtrated using a 0.22 μm nylon syringe filter. Then, the sample was analyzed using HPLC-DAD (the absorbance was measured at 210 nm) and HPLC-RID with Hi-Plex H column (Agilent) using 0.01 M H_2SO_4 as a mobile phase (isocratic mode, with a flow rate of 0.3 mL/min (the total time of 30 min).

4. Investigation of pH, temperature and air tolerance of hydrogen production

To investigate the optimal pH and temperature for hydrogen production, the pUC18-*fd-bcd-T7-etfAB-rnap* plasmid was transformed into *E. coli* K12 W3110 to obtain FBEB-*E. coli*, and grown on an LB agar plate at 37 °C for 16-18 hours in the presence of 100 μg/mL ampicillin. Then, a single colony was inoculated into 5 mL LB broth supplemented with carbon source, trace element and 100 μg/mL ampicillin. The culture was grown at 37 °C for 16-18 hours. Then, the starter was inoculated into 80 mL LB media and induced by adding 1 mM lactose when OD_{600} of the culture reached 0.6-0.8. After the cells were grown for 8 hours with shaking at 37 °C, they were resuspended in the three-component buffer (Tris, MES and acetate) at various pHs (4.5 to 8). After adding 0.4 mmol formate substrate in all reactions, the amount of hydrogen produced was measured at different intervals. To identify the optimal temperature, the hydrogen production at various temperatures (25, 30, 37 and 42 °C) was measured at different time periods.

As *E. coli* is a facultative anaerobe, their ability to tolerate O_2 while still maintaining H_2 production was tested. FBEB-*E. coli* was prepared as described in Section 2 above. Then, the pellet was resuspended in 100 mM potassium phosphate buffer pH 6, and the cells were exposed to air at various time periods (0.5, 1, 2 and 4 hours) before purging the system with N_2 for 30 min. Then, H_2 production by each type of cells at various time periods (0, 1, 2 and 3 hours) was measured in comparison to the condition in which cells were kept anaerobically all the time after the induction. Measurements of H_2 production in the capped vials were done after the anaerobiosis was initiated for 0, 1, 2 and 3 hours. A diagram explaining experimental procedures and the results are shown in Fig. S6.

5. Increasing hydrogen production by removing CO_2 from the system

As CO_2 produced in a 100 mL bottle (closed system) can be accumulated and the high concentration of CO_2 would not favor the forward direction hydrogen production according to thermodynamic principles, we thus adjusted the conditions to lower the gas partial pressure to facilitate hydrogen production. Suspension of FBEB-*E. coli* (60 ml) was prepared as previously mentioned. The cell suspension was adjusted to obtain a final OD_{600} of 2 in 100 mM potassium phosphate buffer, pH 6 and then removed oxygen by equilibrating the solution in an anaerobic glovebox. Formate (0.4 mmol) was added to initiate the reaction. The bottle was connected to another trapping apparatus to allow gases produced (H_2 and CO_2) to pass through a solution of 20 mmol calcium hydroxide to trap CO_2 in the form of $CaCO_3$ (see **Fig. S4**). Therefore, the headspace of the first chamber and the calcium hydroxide trap contained mainly hydrogen as a gas product. Hydrogen and formate were analyzed using GC-TCD and HPLC-DAD, respectively while a total gas volume in the last chamber was measured using a gas-water substitution method.

Author Information
Corresponding Author
*E-mail: pimchai.chaiyen@vistec.ac.th

Notes
A patent related to this work has been filed.

Methods Summary
A full description of the methods can be found in Supporting Information.

Author contributions
Conceptualization: PC
Methodology: PI, CS, AW, JP, JJ, ST, CT, JS, PC
Investigation: PI, CS, AW, JP, JJ, ST, TW, WO
Supervision: PC, JS, TWongnate, NW, AS
Writing– original draft: PI, PC
Writing– review& editing: PI, ST, AS, WB, TWongnate, NW, JS, PC

References

1   Yan, J. Negative-emissions hydrogen energy. *Nature Climate Change* **8**, 560-561, doi:10.1038/s41558-018-0215-9 (2018).

2   Nikolaidis, P. & Poullikkas, A. A comparative overview of hydrogen production processes. *Renewable and Sustainable Energy Reviews* **67**, 597-611, doi:https://doi.org/10.1016/j.rser.2016.09.044 (2017).

3   Staffell, I. *et al.* The role of hydrogen and fuel cells in the global energy system. *Energy & Environmental Science* **12**, 463-491, doi:10.1039/C8EE01157E (2019).

4   Hydrogen generation by market size, share & COVID impact analysis, by type (on-site and portable), by technology (stream methane reforming, water electrolysis, partial oil oxidation, and coal gasification), by application (ammonia production, petroleum refinery, methanol production, transportation, power generation, and others), and regional forecast, 2021-2028. (https://www.fortunebusinessinsights.com/industry-reports/hydrogen-generation-market-100745, 2021).

5   Aireddy, D. R. & Ding, K. Heterolytic Dissociation of H_2 in Heterogeneous Catalysis. *ACS Catalysis* **12**, 4707-4723, doi:10.1021/acscatal.2c00584 (2022).

6   Hand, E. *HIDDEN HYDROGEN Does Earth hold vast stores of a renewable, carbon-free fuel?*, <https://www.science.org/content/article/hidden-hydrogen-earth-may-hold-vast-stores-renewable-carbon-free-fuel> (2023).

7   Lee, S. Y. *et al.* A comprehensive metabolic map for production of bio-based chemicals. *Nature Catalysis* **2**, 18-33, doi:10.1038/s41929-018-0212-4 (2019).

8   Intasian, P. *et al.* Enzymes, In Vivo Biocatalysis, and Metabolic Engineering for Enabling a Circular Economy and Sustainability. *Chemical Reviews* **121**, 10367-10451, doi:10.1021/acs.chemrev.1c00121 (2021).

9   Appel, A. M. *et al.* Frontiers, Opportunities, and Challenges in Biochemical and Chemical Catalysis of CO_2 Fixation. *Chemical Reviews* **113**, 6621-6658, doi:10.1021/cr300463y (2013).

10   Kanygin, A. *et al.* Rewiring photosynthesis: a photosystem I-hydrogenase chimera that makes H_2 *in vivo*. *Energy & Environmental Science* **13**, 2903-2914, doi:10.1039/C9EE03859K (2020).

11   Appel, J., Hueren, V., Boehm, M. & Gutekunst, K. Cyanobacterial in vivo solar hydrogen production using a photosystem I–hydrogenase (PsaD-HoxYH) fusion complex. *Nature Energy* **5**, 458-467, doi:10.1038/s41560-020-0609-6 (2020).

12   Evans, R. M. *et al.* Mechanistic Exploitation of a Self-Repairing, Blocked Proton Transfer Pathway in an O_2-Tolerant [NiFe]-Hydrogenase. *Journal of the American Chemical Society* **140**, 10208-10220, doi:10.1021/jacs.8b04798 (2018).

13   Ragsdale, S. W. Nickel-based Enzyme Systems *Journal of Biological Chemistry* **284**, 18571-18575, doi:10.1074/jbc.R900020200 (2009).

14   Zhou, J., Liu, L., Shi, Z., Du, G. & Chen, J. ATP in current biotechnology: regulation, applications and perspectives. *Biotechnol Adv* **27**, 94-101, doi:10.1016/j.biotechadv.2008.10.005 (2009).

15   Maeda, T., Sanchez-Torres, V. & Wood, T. K. Hydrogen production by recombinant *Escherichia coli* strains. *Microb Biotechnol* **5**, 214-225, doi:10.1111/j.1751-7915.2011.00282.x (2012).

16   Thakker, C., Martínez, I., San, K.-Y. & Bennett, G. N. Succinate production in *Escherichia coli*. *Biotechnol J* **7**, 213-224, doi:10.1002/biot.201100061 (2012).

17   Buckel, W. & Thauer, R. K. Flavin-Based Electron Bifurcation, A New Mechanism of Biological Energy Coupling. *Chemical Reviews* **118**, 3862-3886, doi:10.1021/acs.chemrev.7b00707 (2018).

18   Sucharitakul, J., Buckel, W. & Chaiyen, P. Rapid kinetics reveal surprising flavin chemistry in bifurcating electron transfer flavoprotein from Acidaminococcus fermentans. *Journal of Biological Chemistry* **296**, doi:10.1074/jbc.RA120.016017 (2021).

19   McDowall, J. S. *et al.* Bacterial formate hydrogenlyase complex. *Proceedings of the National Academy of Sciences* **111**, E3948-E3956, doi:doi:10.1073/pnas.1407927111 (2014).

20   Sucharitakul, J. *et al.* Modulations of the reduction potentials of flavin-based electron bifurcation complexes and semiquinone stabilities are key to control directional electron flow. *The FEBS Journal* **288**, 1008-1026, doi:https://doi.org/10.1111/febs.15343 (2021).

21   Maeda, T., Sanchez-Torres, V. & Wood, T. K. Metabolic engineering to enhance bacterial hydrogen production. *Microb Biotechnol* **1**, 30-39, doi:https://doi.org/10.1111/j.1751-7915.2007.00003.x (2008).

22   Fan, Z., Yuan, L. & Chatterjee, R. Increased Hydrogen Production by Genetic Engineering of Escherichia coli. *PLOS ONE* **4**, e4432, doi:10.1371/journal.pone.0004432 (2009).

23   Youcai, Z. & Tao, Z. in *Biohydrogen Production and Hybrid Process Development* (eds Zhao Youcai & Zhou Tao) 1-24 (Elsevier, 2021).

24   Graef, M. R. d., Alexeeva, S., Snoep, J. L. & Mattos, M. J. T. d. The Steady-State Internal Redox State (NADH/NAD) Reflects the External Redox State and Is Correlated with Catabolic Adaptation in Escherichia coli. *Journal of Bacteriology* **181**, 2351-2357, doi:doi:10.1128/JB.181.8.2351-2357.1999 (1999).

25   Blbulyan, S. & Trchounian, A. Impact of membrane-associated hydrogenases on the FOF1-ATPase in *Escherichia coli* during glycerol and mixed carbon fermentation: ATPase activity and its inhibition by N,N′-dicyclohexylcarbodiimide in the mutants lacking hydrogenases. *Archives of Biochemistry and Biophysics* **579**, 67-72, doi:https://doi.org/10.1016/j.abb.2015.05.015 (2015).

26   Yang, C. *et al.* Engineering an efficient H_2 utilizing *Escherichia coli* platform by modulation of endogenous hydrogenases. *Biochemical Engineering Journal* **166**, 107851, doi:https://doi.org/10.1016/j.bej.2020.107851 (2021).

27   Dong, H. *et al.* in *Bioreactor Engineering Research and Industrial Applications I: Cell Factories* (eds Qin Ye, Jie Bao, & Jian-Jiang Zhong) 141-163 (Springer Berlin Heidelberg, 2016).

28   Gulevich, A. Y., Skorokhodova, A. Y., Sukhozhenko, A. V., Shakulov, R. S. & Debabov, V. G. Metabolic engineering of *Escherichia coli* for 1-butanol biosynthesis through the inverted aerobic fatty acid β-oxidation pathway. *Biotechnol Lett* **34**, 463-469, doi:10.1007/s10529-011-0797-z (2012).

29   Seregina, T. A., Shakulov, R. S., Debabov, V. G. & Mironov, A. S. Construction of a butyrate-producing *E. coli* strain without the use of heterologous genes. *Applied Biochemistry and Microbiology* **46**, 745-754, doi:10.1134/S000368381008003X (2010).

30   Haller, T., Buckel, T., Rétey, J. & Gerlt, J. A. Discovering New Enzymes and Metabolic Pathways: Conversion of Succinate to Propionate by *Escherichia coli*. *Biochemistry* **39**, 4622-4629, doi:10.1021/bi992888d (2000).

31   Xiao, W., Wang, R. S., Handy, D. E. & Loscalzo, J. NAD(H) and NADP(H) Redox Couples and Cellular Energy Metabolism. *Antioxid Redox Signal* **28**, 251-272, doi:10.1089/ars.2017.7216 (2018).

32   Riondet, C., Cachon, R., Waché, Y., Alcaraz, Gérard & Diviès, C. Changes in the proton-motive force in Escherichia coli in response to external oxidoreduction potential. *European Journal of Biochemistry* **262**, 595-599, doi:https://doi.org/10.1046/j.1432-1327.1999.00429.x (1999).

33   Mathews, J., Li, Q. & Wang, G. Characterization of hydrogen production by engineered Escherichia coli strains using rich defined media. *Biotechnology and Bioprocess Engineering* **15**, 686-695, doi:10.1007/s12257-009-3139-4 (2010).

34   Pinhal, S., Ropers, D., Geiselmann, J., Jong, H. d. & Metcalf, W. W. Acetate Metabolism and the Inhibition of Bacterial Growth by Acetate. *Journal of Bacteriology* **201**, e00147-00119, doi:doi:10.1128/JB.00147-19 (2019).

35   Szenk, M., Dill, K. A. & de Graff, A. M. R. Why Do Fast-Growing Bacteria Enter Overflow Metabolism? Testing the Membrane Real Estate Hypothesis. *Cell Syst* **5**, 95-104, doi:10.1016/j.cels.2017.06.005 (2017).

36   Clark, D. P. The fermentation pathways of Escherichia coli. *FEMS Microbiology Letters* **63**, 223-234, doi:https://doi.org/10.1016/0378-1097(89)90132-8 (1989).

37   Choi, C. *17% of food production globally wasted, UN report estimates*, <https://www.wfp.org/stories/5-facts-about-food-waste-and-hunger> (2021).

38   *Landfill Methane Outreach Program (LMOP)*, <https://www.epa.gov/lmop/basic-information-about-landfill-gas> (2021).

39   Wang, J. & Yin, Y. *Clostridium* species for fermentative hydrogen production: An overview. *International Journal of Hydrogen Energy* **46**, 34599-34625, doi:https://doi.org/10.1016/j.ijhydene.2021.08.052 (2021).

40   Dutta, D., De, D., Chaudhuri, S. & Bhattacharya, S. K. Hydrogen production by Cyanobacteria. *Microbial Cell Factories* **4**, 36, doi:10.1186/1475-2859-4-36 (2005).

41   Silva, P. J. *et al.* Enzymes of hydrogen metabolism in *Pyrococcus furiosus*. *Eur J Biochem* **267**, 6541-6551, doi:10.1046/j.1432-1327.2000.01745.x (2000).

42   Lamont, C. M. *et al.* Expanding the substrates for a bacterial hydrogenlyase reaction. *Microbiology* **163**, 649-653, doi:https://doi.org/10.1099/mic.0.000471 (2017).

43   Trchounian, A. A., Bagramyan, K. A., Vassilian, A. V. & Poladian, A. A. Relationship between formate hydrogen lyase and proton-potassium pump under heterolactic fermentation in *Escherichia coli*: functional multienzyme associations in the cell membrane. *Membr Cell Biol* **13**, 511-526 (2000).

44   Gevorgyan, H., Trchounian, A. & Trchounian, K. Understanding the Role of *Escherichia coli* Hydrogenases and Formate Dehydrogenases in the FOF1-ATPase Activity during the Mixed Acid Fermentation of Mixture of Carbon Sources. *IUBMB Life* **70**, 1040-1047, doi:https://doi.org/10.1002/iub.1915 (2018).

45   Jaroensuk, J., Chuaboon, L. & Chaiyen, P. Biochemical reactions for in vitro ATP production and their applications. *Molecular Catalysis* **537**, 112937, doi:https://doi.org/10.1016/j.mcat.2023.112937 (2023).

46   Hara, K. Y. & Kondo, A. ATP regulation in bioproduction. *Microbial cell factories* **14**, 198-198, doi:10.1186/s12934-015-0390-6 (2015).

47   Bozell, J. J. & Petersen, G. R. Technology development for the production of biobased products from biorefinery carbohydrates—the US Department of Energy's "Top 10" revisited. *Green Chemistry* **12**, 539-554, doi:10.1039/B922014C (2010).

48   Ahn, J. H., Jang, Y.-S. & Lee, S. Y. Production of succinic acid by metabolically engineered microorganisms. *Current Opinion in Biotechnology* **42**, 54-66, doi:https://doi.org/10.1016/j.copbio.2016.02.034 (2016).

49   Bradfield, M. F. A. *et al.* Continuous succinic acid production by *Actinobacillus succinogenes* on xylose-enriched hydrolysate. *Biotechnology for Biofuels* **8**, 181, doi:10.1186/s13068-015-0363-3 (2015).

50   Scholten, E., Renz, T. & Thomas, J. Continuous cultivation approach for fermentative succinic acid production from crude glycerol by *Basfia succiniciproducens* DD1. *Biotechnology Letters* **31**, 1947, doi:10.1007/s10529-009-0104-4 (2009).